Development 130, 2917-2928

doi:10.1242/dev.00511

Alx1, a member of the Cart1/Alx3/Alx4 subfamily of Paired-class homeodomain proteins, is an essential component of the gene network controlling skeletogenic fate specification in the sea urchin embryo

Charles A. Ettensohn[1,*], Michele R. Illies[1], Paola Oliveri[2] and Deborah L. De Jong[1]

[1]Department of Biological Sciences, Carnegie Mellon University, 4400 Fifth Avenue, Pittsburgh, PA 15213, USA
[2]Division of Biology, California Institute of Technology, Pasadena, CA 91125, USA
*Author for correspondence (e-mail: ettensohn@andrew.cmu.edu)

Accepted 27 March 2003

SUMMARY

In the sea urchin embryo, the large micromeres and their progeny function as a critical signaling center and execute a complex morphogenetic program. We have identified a new and essential component of the gene network that controls large micromere specification, the homeodomain protein Alx1. Alx1 is expressed exclusively by cells of the large micromere lineage beginning in the first interphase after the large micromeres are born. Morpholino studies demonstrate that Alx1 is essential at an early stage of specification and controls downstream genes required for epithelial-mesenchymal transition and biomineralization. Expression of Alx1 is cell autonomous and regulated maternally through β-catenin and its downstream effector, Pmar1. Alx1 expression can be activated in other cell lineages at much later stages of development, however, through a regulative pathway of skeletogenesis that is responsive to cell signaling. The Alx1 protein is highly conserved among euechinoid sea urchins and is closely related to the Cart1/Alx3/Alx4 family of vertebrate homeodomain proteins. In vertebrates, these proteins regulate the formation of skeletal elements of the limbs, face and neck. Our findings suggest that the ancestral deuterostome had a population of biomineral-forming mesenchyme cells that expressed an Alx1-like protein.

Key words: Sea urchin embryo, Early development, Fate specification, Skeletogenesis, Primary mesenchyme cells, Alx1, Cart1, Biomineralization, Epithelial-mesenchymal transition, Alx3, Alx4

INTRODUCTION

The primary mesenchyme cell (PMC) lineage of the sea urchin embryo is a model system for the analysis of fate specification, cell signaling, morphogenesis and biomineralization. PMCs are derived from the micromeres of the 16-cell stage embryo. At the fifth cleavage division, the micromeres divide unequally. The four large daughter cells (large micromeres) are the founder cells of the primary mesenchyme and the small daughter cells (small micromeres) contribute to the coelomic pouches. Isolation and transplantation of micromeres or large micromeres from early cleavage stage embryos show that these cells are autonomously programmed to give rise to skeletogenic cells and that all but the most terminal aspects of their differentiation program are insensitive to extrinsic cues (see Ettensohn and Sweet, 2000; Brandhorst and Klein, 2002; Angerer and Angerer, 2003). Cell division within the micromere territory lags behind the remainder of the embryo and the small micromeres divide even more slowly than the large micromeres. This temporal pattern of cleavage generates transient 56- and 60-cell stages (Summers et al., 1993). By the late blastula stage, the large micromeres have divided two to three times depending on the species, and their 16 or 32 progeny are positioned at the vegetal pole in a ring that surrounds the small micromere descendants. The large micromere progeny undergo an epithelial-mesenchymal transition at the beginning of gastrulation and ingress into the blastocoel, forming the primary mesenchyme. During gastrulation and later development, PMCs migrate to specific target sites along the blastocoel wall and secrete the calcified endoskeleton of the larva.

Recent studies have begun to elucidate the gene regulatory network that underlies PMC specification. The initial specification of the large micromere lineage is entrained by a patterning system linked to the animal-vegetal polarity of the unfertilized egg (Ettensohn and Sweet, 2000; Brandhorst and Klein, 2002; Angerer and Angerer, 2003). One important component of this system is β-catenin. β-catenin is localized in the nuclei of vegetal blastomeres during early cleavage and becomes concentrated at the highest levels in the micromere lineage (Logan et al., 1999). Nuclearization of β-catenin is required for all known aspects of mesoderm and endoderm formation, including large micromere specification (Emily-Fenouil et al., 1998; Wikramanayake et al., 1998; Logan et al., 1999; Davidson et al., 2002). This indicates that β-catenin, in combination with its LEF/TCF partner(s) (Huang

et al., 2000; Vonica et al., 2000), provides a very early input into the PMC gene network. One critical early target of β-catenin is the transcriptional repressor Pmar1 (Oliveri et al., 2002). Pmar1 is transiently expressed in both large and small micromeres during early development. In the large micromeres, Pmar1 is thought to block the expression of an unknown, global repressor of PMC specification. As a consequence of these early molecular events, other transcriptional regulators are activated selectively in the large micromere lineage later in development, including Ets1 (Kurokawa et al., 1999) and Tbr (Croce et al., 2001; Fuchikami et al., 2002). Presumably, these and other transcription factors control the expression of downstream genes that regulate primary mesenchyme morphogenesis and biomineralization (Zhu et al., 2001; Illies et al., 2002), although these links have not been established.

During normal embryogenesis, only the large micromeres give rise to skeleton-forming cells. Under experimental conditions, however, the same developmental program can be activated in other cell lineages. Removal of micromeres at the 16-cell stage or PMCs at the early gastrula stage leads to the transfating of macromere-derived cells (secondary mesenchyme cells, or SMCs) to the PMC fate (Ettensohn, 1992; Sweet et al., 1999). The transfating cells exhibit all features of the PMC phenotype that have been examined. They express PMC-specific molecular markers (including MSP130, SM50, and SM30), migrate to PMC-specific target sites, acquire PMC-specific signaling properties, and synthesize a normally patterned skeleton (Ettensohn and McClay, 1988; Ettensohn and Ruffins, 1993; Guss, 1997).

In this study, we have identified a new and essential component of the PMC gene network, Alx1. We show that Alx1 protein is required for an early step in the specification of the large micromere lineage and for the transfating of non-micromere-derived cells to a PMC fate. Alx1 is the first known invertebrate member of the Cart1/Alx3/Alx4 subfamily of Paired class homeodomain proteins. As these proteins have been shown to function in skeletogenesis in vertebrates, our findings have implications concerning the evolution of biomineralization within the deuterostomes.

MATERIALS AND METHODS

Animals

Adult *Strongylocentrotus purpuratus* were obtained from Marinus, Inc. (Long Beach, CA, USA) and Pat Leahy (Kerchoff Marine Laboratory, California Institute of Technology, USA). Adult *Lytechinus variegatus* were obtained from the Duke University Marine Laboratory (Beaufort, NC, USA) and Carolina Biological Supply (Burlington, NC, USA). Spawning was induced by intracoelomic injection of 0.5 M KCl and embryos were cultured in artificial seawater (ASW) in temperature-controlled incubators (*L. variegatus*, 23°C; *S. purpuratus*, 15.5°C).

Whole-mount in situ hybridization

In situ hybridization was carried out according to the method of Zhu et al. (Zhu et al., 2001). SpAlx1 probe was generated from clone 16-I18 (a full-length clone) and LvAlx1 probe was generated from a 3.2 kb cDNA that included the C-terminal third of the protein-coding sequence and most of the 3′-UTR.

Morpholino antisense oligonucleotides (MO) and mRNA injections

Fertilized *L. variegatus* eggs were injected as described previously (Sweet et al., 2002). *S. purpuratus* eggs were dejellied by incubating for 10 minutes in pH 5.0 ASW before being placed in rows on protamine sulfate-coated dishes. Eggs were fertilized on the dishes and injected within 5 minutes. LvAlx1 MO was complementary to the 5′ end of the coding region and had the sequence ACGGCATTGACG-GGTAGAATAACAT. SpAlx1 MO was complementary to the 5′-UTR and had the sequence TATTGAGTTAAGTCTCGGCACGACA. For most experiments, MO injection solutions contained 2 mM LvAlx1 or SpAlx1 MO, 20% glycerol (vol/vol), and 0.1% rhodamine dextran (wt/vol).

Alx1 antibody production and immunostaining

A DNA fragment corresponding to amino acids 242-369 of LvAlx1 was subcloned into pET32 (Novagen, Madison, WI) to create a histidine-tagged, thioredoxin-fusion protein. The fusion protein was purified from *E. coli* using a nickel column (Novagen) and then used to generate a rabbit polyclonal antibody (Pocono Rabbit Farm and Laboratory, Canadensis, PA). For Alx1 immunostaining, embryos were fixed in fresh 2% paraformaldehyde in ASW for 20 minutes at room temperature. After rinsing once with ASW, the embryos were postfixed/permeabilized with 100% methanol (5 minutes at –20°C). For staining with 6a9, Endo1 or anti-myosin, embryos were fixed in methanol alone. Embryos were washed 3× with PBS and incubated in 4% goat serum in PBS (PBS-GS) for 30 minutes. They were transferred to flexible, round-bottom 96-well plates and staining was carried out as described by Hodor et al. (Hodor et al., 2000). Primary antibodies were crude LvAlx1 antiserum or preimmune serum (1:100 in PBS-GS), mAbs 6a9 and Endo1 (full-strength tissue culture supernatants), and anti-myosin (1:100 in PBS-GS). Secondary antibodies were fluorescein-conjugated, goat anti-rabbit IgG or fluorescein-conjugated, goat anti-mouse IgG+IgM (Cappel, ICN Biomedicals) (1:50 in PBS-GS). For double staining experiments, embryos that had been stained with LvAlx1 antiserum and fluorescein-conjugated secondary antibody were washed as described by Hodor et al. (Hodor et al., 2000) and incubated overnight at 4°C with full-strength monoclonal antibody 6a9. The embryos were washed again, incubated for 2-4 hours at room temperature in affinity-purified, Texas red-conjugated goat anti-mouse IgG/IgM (H+L) (Jackson Immunoresearch) (1:50 in PBS-GS), washed and mounted.

Quantitative PCR (QPCR)

Total RNA was isolated from control (uninjected) and experimental embryos (injected with a 200 μM injection solution of MO or 2 mg/ml mRNA injection solution) using RNAzol (Leedo Medical Laboratories, Houston, TX). DNA-Free (Ambion) was used to eliminate contaminating DNA. First-strand cDNA was synthesized with RNA extracted from 200-300 embryos using random hexamers and the Taq Man kit (PE Biosystems). cDNA was diluted to a concentration of 1 embryo/μl. Specific primer sets for each gene were designed using the known cDNA sequences and the program Primer3 (Rozen and Skaletsky, 2000) (publicly available at www.genome.wi.mit.edu/genome_software/other/primer3). Primer sets were chosen to amplify products 100-200 bp in length. Reactions were carried out in triplicate using cDNA from 2 embryos/reaction as template and SYBR green chemistry (PE Biosystems). Thermal cycling parameters were as described previously (Rast et al., 2000) and data were analyzed using an ABI 5700 sequence detection system. The average of data for the three cycles at the threshold (C_T) for each gene was normalized against the average C_T for ubiquitin mRNA, which is known to be expressed at constant levels during the first 24 hours of development. Primer efficiencies (i.e., the amplification factors for each cycle) were found to exceed 1.9. Relative folds of difference between control and experimental embryos were calculated (see Tables 1 and 2). In every experiment, a no-template control was

included for each set of primers. Each experiment also included a control comparing levels of test mRNAs in uninjected embryos and embryos injected with a control MO. Data were only included when no more than one cycle of difference was observed for each mRNA tested.

PMC removal

PMCs were removed from mesenchyme blastula stage embryos as described previously (Ettensohn and McClay, 1988).

RESULTS

Cloning and sequence analysis of SpAlx1 and LvAlx1

In a previous large-scale cDNA sequencing analysis we identified a cDNA clone (16-I18) from *S. purpuratus* that encoded a protein similar to *Drosophila* Aristaless and related proteins in vertebrates (Zhu et al., 2001). We sequenced both strands of this full-length clone and determined the predicted amino acid sequence of the protein (Fig. 1A; GenBank accession no. AY277399). Although this protein was originally named SpAristaless, we changed the name to SpAlx1 to reflect the evolutionary conservation of the homeodomain of the sea urchin protein with the vertebrate aristaless-like homeobox proteins Alx3 and Alx4 (see below). RT-PCR and RACE were used to clone an orthologous gene product from *L. variegatus*, a species separated from *S. purpuratus* by 30-40 million years (Smith, 1988) (Fig. 1A; GenBank accession no. AY277400). ClustalX alignment shows that the LvAlx1 and SpAlx1 proteins have an overall amino acid identity of 95%. The two mRNAs are highly conserved at the nucleotide level in both coding and non-coding regions (see GenBank nucleotide entries).

Alx1 contains a homeodomain, the sequence of which is identical in *L. variegatus* and *S. purpuratus* (Fig. 1A). Analysis of this 60-amino acid sequence showed that it contains several signature residues characteristic of a Paired-class homeodomain (Galliot et al., 1999; Banerjee-Basu and Baxevanis, 2001). Paired-class homeodomain sequences have been further grouped into 18 distinct subfamilies (Galliot et al., 1999). Analysis of the Sp/LvAlx1 homeodomain using ClustalX and PAUP showed that this sequence is most closely related to the homeodomains of the Cart1/Alx3/Alx4 subfamily (Fig. 1B). Alx1 is the first invertebrate member of this subfamily. Alx1 and the vertebrate members of the subfamily lack a Paired domain, a distinct DNA-binding domain found in some proteins that also contain a Paired-class homeodomain.

SpAlx1 and LvAlx1 also contain a perfectly conserved C-terminal OAR (otp, aristaless, Rx) domain (Fig. 1A). Many Paired-class homeodomain proteins, including members of the Cart1/Alx3/Alx4 subfamily, have an OAR domain at the C terminus (Gaillot et al., 1999). The function of this domain is poorly understood, although it may bind to and mask transactivation domains located elsewhere in the proteins, a masking effect that can be relieved by the binding of other proteins to the OAR domain (Amendt et al., 1999; Norris and Kern, 2001; Brouwer et al., 2003).

Except within the homeodomain and OAR domain, SpAlx1 and LvAlx1 show no significant similarities to other proteins by BLAST analysis. We noted, however, a 25-30 amino acid region immediately upstream of the homeodomain that contains a high number of charged residues (aspartic acid and lysine; Fig. 1A), a feature shared by the vertebrate Alx4 and Cart1 proteins. Moreover, SpAlx1 and LvAlx1 are proline-rich (12% proline residues outside the OAR domain and homeodomain), another characteristic of the vertebrate Alx3 and Alx4 proteins.

Developmental expression of Alx1 mRNA and protein

Northern blot analysis with a full-length probe complementary to *Spalx1* revealed a single major transcript with an apparent length of 5-5.5 kb (not shown). This corresponded well to the predicted size of the *Spalx1* mRNA based on the sequence of clone 16-I18 (~5 kb). *Spalx1* mRNA was not detectable in the unfertilized egg or at very early cleavage stages by northern analysis, but was strongly expressed by the blastula stage.

Whole-mount in situ hybridization showed that *Spalx1* mRNA was expressed specifically by cells of the large micromere-PMC lineage (Fig. 2). Expression was first detectable as one to two distinct intranuclear spots of staining in each of the four large daughter cells of the micromeres at the 56-cell stage. At this stage of development, most of the cells of the embryo have undergone the sixth cleavage division but the micromeres have divided only once, producing four large and four small daughter cells. *Spalx1* mRNA accumulated only in the large daughter cells, the founder cells of the PMC lineage, beginning in the first interphase after these cells were born. After the next cell division, *Spalx1* mRNA was detectable at higher levels in all eight large micromere progeny. Intense signal was evident during the blastula stage in presumptive PMCs. *Spalx1* mRNA was expressed specifically by PMCs throughout gastrulation and later embryogenesis, although levels gradually decreased. Faint expression in PMCs was still evident at the early pluteus stage, the latest developmental stage examined.

In *L. variegatus*, expression of *alx1* mRNA was also restricted to the large micromere-PMC lineage (Fig. 2). Expression was delayed slightly relative to *S. purpuratus* when assayed by in situ hybridization. *Lvalx1* mRNA was first detectable in some embryos in the eight daughter cells of the large micromeres at ~5 hours postfertilization (~128-cell stage). The transcript was expressed at high levels in the large micromere progeny after these cells had undergone one additional division; i.e. in the 16 descendants of the large micromeres. As in *S. purpuratus*, levels of expression were high in PMCs following ingression and then gradually declined during later development. *Lvalx1* expression was not detectable in most embryos after the late gastrula stage. The *Lvalx1* probe showed the same pattern of hybridization when used to probe embryos of *L. pictus*, indicating that the *alx1* gene is also conserved in this species and is expressed in a similar fashion (not shown).

A polyclonal antiserum was generated against a 128-amino acid region in the C-terminal half of LvAlx1 (see Materials and Methods). This antibody cross-reacted with SpAlx1, probably because of the high degree of conservation between the two proteins. The anti-Alx1 antiserum specifically labeled the nuclei of cells of the large micromere-PMC lineage (Fig. 3). In *L. variegatus*, nuclear staining was evident at the

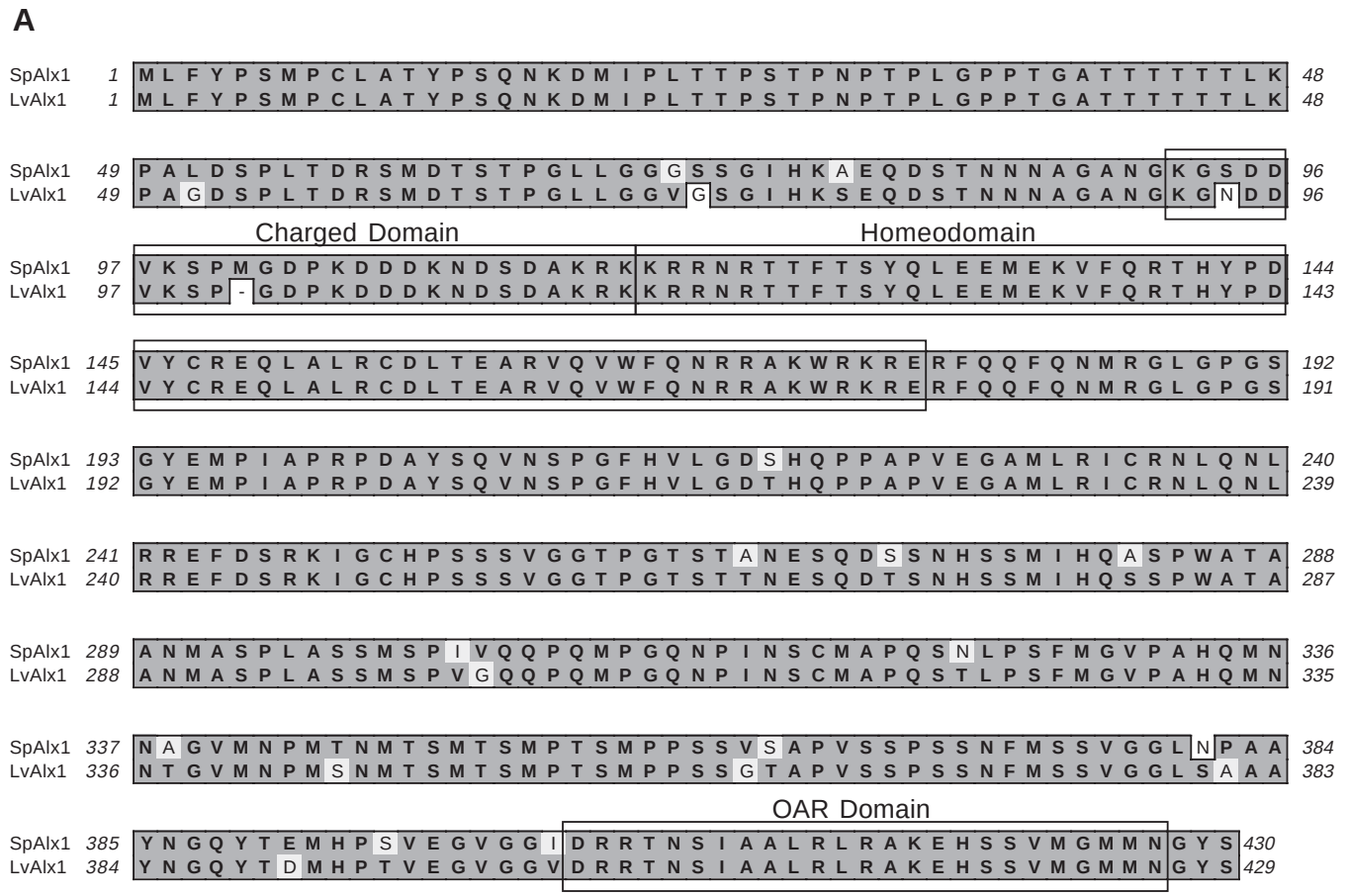

Fig. 1. (A) ClustalX alignment of the predicted amino acid sequences of SpAlx1 and LvAlx1. Homeodomains, OAR domains, and charged domains are boxed. Note that in each case the assignment of the start methionine is provisional, as there are three in-frame AUG codons near the 5′ end of the open reading frame (ORF) of each mRNA. There are in-frame stop codons upstream of each ORF. (B) Unrooted neighbor-joining tree showing the relationship of Lv/SpAlx1 to other Paired-class proteins (homeodomains only). The other proteins shown are those with Paired-class homeodomains that are most closely related to those of the Cart1/Alx3/Alx4 subfamily (Galliot et al., 1999). A multiple alignment was generated using ClustalX and tree construction was carried out with PAUP*4.0 (Sinauer Associates) using the Neighbor Joining Method. Numbers indicate the fraction of amino acid substitutions between nodes.

blastula stage prior to PMC ingression and PMC nuclei were labeled throughout gastrulation. Double-labeling with the PMC-specific monoclonal antibody (mAb) 6a9 confirmed that the Alx1-expressing cells were PMCs (Fig. 3G). Nuclear staining of PMCs was still evident at the early pluteus stage, the latest developmental stage examined. In *S. purpuratus*, the earliest stage at which we could reliably detect nuclear localization of Alx1 was in the interphase following the first division of the large micromeres, i.e., when there were eight large micromere progeny (Fig. 6A). This was one cell division later than *Spalx1* mRNA expression was first detectable by in situ hybridization and may reflect a lag between transcriptional activation of the *Spalx1* gene and the accumulation of sufficient amounts of protein to be detected by immunostaining.

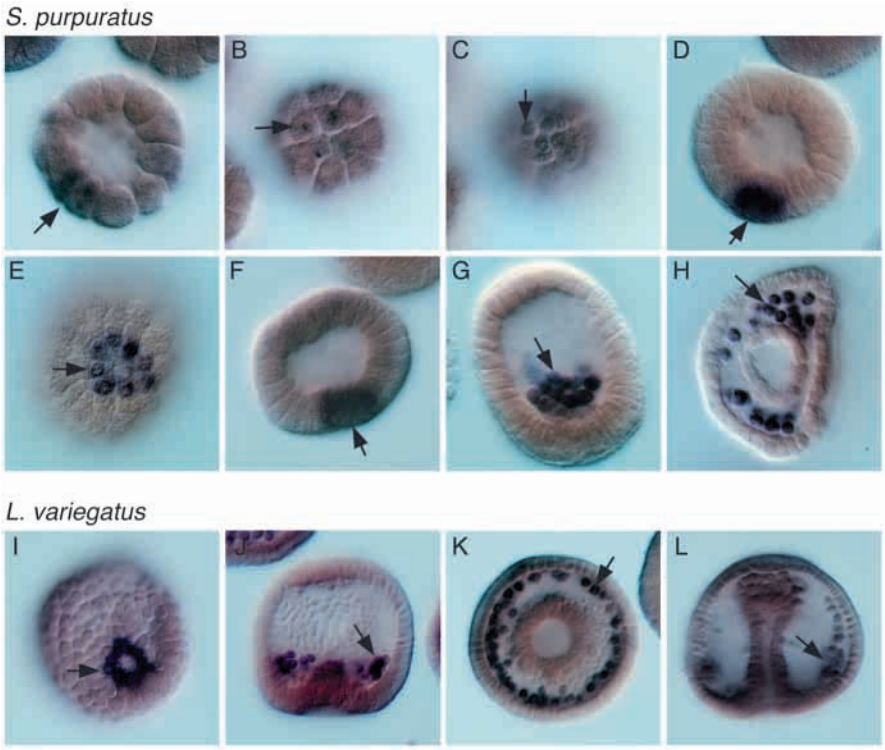

Fig. 2. Whole-mount in situ hybridizations showing *alx1* mRNA expression in *S. purpuratus* (A-H) and *L. variegatus* (I-L) embryos. (A) 56-cell stage embryo, the earliest stage at which *alx1* mRNA is detectable in the four large micromeres (arrow). Initially, staining is limited to one to two small, intracellular spots in each cell. (B,C) Two focal planes of a 56-cell stage embryo, viewed along the animal-vegetal axis. *Alx1* mRNA is present in the large micromeres (B, arrow) but not the small micromeres (C, arrow). (D,E) Lateral and vegetal views, respectively, of ~128-cell stage embryos, showing *alx1* mRNA in the eight progeny of the large micromeres (arrows). (F) Mid-blastula stage. (G) Mesenchyme blastula. (H) Late gastrula. *Alx1* transcript continues to be restricted to large micromere progeny throughout blastula and gastrula stages (arrows). In *L. variegatus*, *alx1* is expressed in a similar pattern, although expression is first detectable, by in situ hybridization, one cell cycle later than in *S. purpuratus*, after the large micromeres have divided once. (I) Blastula, showing expression in ~16 large micromere progeny (arrow). (J) Early gastrula. (K) Mid-gastrula. (L) Late gastrula. Alx1-expressing PMCs are indicated by arrows. By the end of gastrulation, levels of *Lvalx1* expression have declined in most embryos.

The role of Alx1 in PMC specification

To determine the function of Alx1 in PMC specification, we injected morpholino antisense oligonucleotides (MOs) complementary to *alx1* mRNA into fertilized eggs of *S. purpuratus* and *L. variegatus*. SpAlx1 and LvAlx1 MOs were designed to be complementary to non-overlapping regions of the respective mRNAs. The SpAlx1 MO was targeted against the 5′-UTR, while the LvAlx1 MO was complementary to the 5′ end of the coding region, including the putative start codon (see Materials and Methods).

The phenotypes of MO-injected *S. purpuratus* and *L. variegatus* embryos were essentially identical (Fig. 4). Development appeared normal during cleavage and blastula stages, and injected embryos hatched within 1 hour of sibling controls (*L. variegatus*, 23°C). At the late blastula stage, however, a striking phenotype became apparent. PMCs did not ingress in the MO-injected embryos and invagination of the vegetal plate was delayed by several hours relative to control sibling embryos. MO-injected embryos failed to form visible skeletal elements even after extended periods of culture (3 and 6 days for *L. variegatus* and *S. purpuratus*, respectively) (Fig. 4).

By co-injecting fluorescent dextran with the MOs, we observed that the severity of the phenotype depended on the amount of MO injected. Eggs that were injected with larger volumes of 2 mM MO solution (5-10 pl) showed the most extreme phenotype; i.e., a complete lack of PMCs/skeletal elements and delayed invagination. Those injected with smaller volumes (2-5 pl) showed a partial phenotype; i.e., reduced numbers of PMCs, small skeletal elements, and only a slight delay in invagination. In most of our experiments, we used levels of MO sufficient to produce the extreme phenotype in >90% of the embryos.

Alx1 MOs interfered with normal PMC specification as assayed by the expression of a battery of molecular markers (Fig. 5, Table 1). mAb 6a9 recognizes PMC-specific cell surface proteins of the MSP130 family (Ettensohn and McClay, 1988; Illies et al., 2002). Alx1 MO-injected *S. purpuratus* and *L. variegatus* embryos had greatly reduced numbers of 6a9-positive cells (Fig. 5G-H; and see below). This effect was dose-dependent; high doses of MO completely blocked the formation of 6a9(+) cells. The expression of *SpMSP130-related 2* (a MSP protein family member), *SpP19* and *SpFRP* (fibrinogen-related protein) (Zhu et al., 2001; Illies et al., 2002) was examined by in situ hybridization (Fig. 5A-F). Most embryos lacked detectable expression of these markers or had greatly reduced numbers of mesenchyme cells that expressed the mRNAs. Finally, in *S. purpuratus* we used QPCR to measure levels of expression of nine genes expressed exclusively or selectively by cells of the large micromere-PMC lineage (Table 1). SpAlx1 MO had no detectable effect on levels of four of the mRNAs: *tbr* (Fuchikami et al., 2002), *ets1* (Kurokawa et al., 1999), *delta* (Sweet et al., 2002) and *pmar1* (Oliveri et al., 2002) when assessed either at 18-20 hours or 23-24 hours post-fertilization. The level of *Spalx1* mRNA was slightly elevated in MO-injected embryos, suggesting that Alx1 protein may act as a negative regulator of the *alx1* gene. Four of the mRNAs we tested, *dri* (G. Amore and E. Davidson, personal communication), *MSP130* (Parr et al., 1990), *MSP130-related 2* (Illies et al., 2002) and *sm50* (Katoh-Fukui et al., 1991), were down-regulated in MO-injected embryos.

Several molecular markers and morphological criteria were used to determine whether cell types other than PMCs were affected by Alx1 MOs. As noted above, invagination was delayed but eventually occurred in the absence of any primary mesenchyme. In the transparent embryos of *L. variegatus*, it

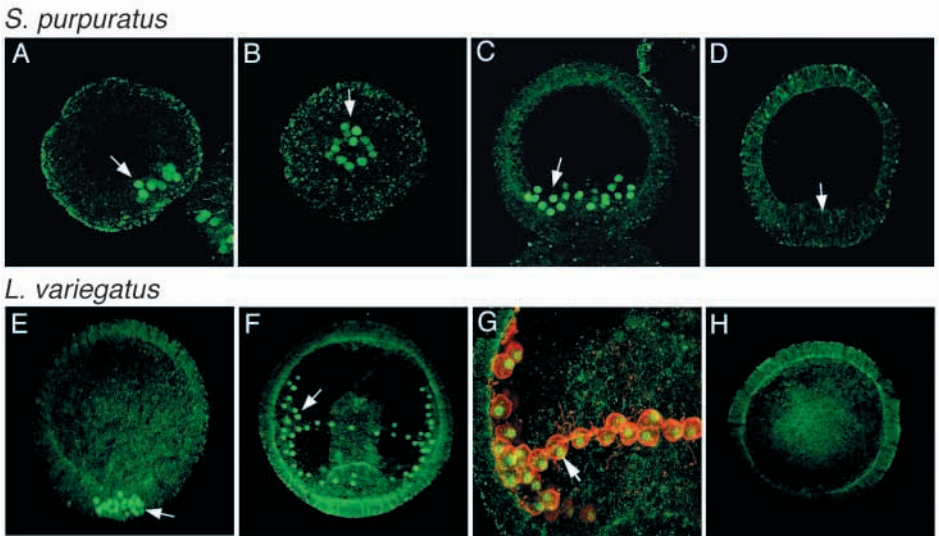

Fig. 3. Alx1 protein expression in *S. purpuratus* (A-D) and *L. variegatus* (E-H) embryos. In both species, Alx1 protein is restricted to the nuclei of large micromere progeny (arrows). Expression is first detectable prior to PMC ingression and is evident throughout gastrulation. (A) 128-cell stage. (B) Mid-blastula stage; vegetal view. (C) Mesenchyme blastula. (D) An Alx1 MO-injected embryo that was allowed to develop until controls had reached the late gastrula stage. No nuclear staining is evident in cells of the vegetal plate (arrow). (E) Blastula. (F) Late gastrula. (G) Late gastrula stained with αAlx1 and mAb 6a9, which recognizes a family of PMC-specific cell surface proteins. There is a one-to-one correspondence between 6a9- and Alx1-positive cells (arrow). (H) Overexpression of *Xenopus* C-cadherin. This embryo was fixed when sibling controls were late gastrulae. It has an animalized phenotype (Wikramanayake et al., 1998; Logan et al., 1999) and no Alx1 staining is detectable.

was evident that the shape of the archenteron was altered in MO-injected embryos. In many embryos, the anterior end was distended and the roof sagged into the lumen of the gut. Nevertheless, the gut became segmented and Endo1, a midgut/hindgut marker (Wessel and McClay, 1985), was eventually expressed in an appropriate pattern (Fig. 5I,J). Large numbers of pigment cells formed in Alx1 MO-injected *L. variegatus* and *S. purpuratus* embryos (Fig. 5M,N). In *S. purpuratus*, these cells stained with the pigment cell-specific antibody Sp1 (Gibson and Burke, 1985; not shown). Several observations showed that Alx1 MOs did not interfere with the normal polarization of the ectoderm along the oral-aboral axis. A morphological difference between squamous aboral and columnar oral ectoderm cells was evident in MO-injected embryos (Fig. 4G,H,P) and pigment cells were restricted to the aboral ectoderm, as in

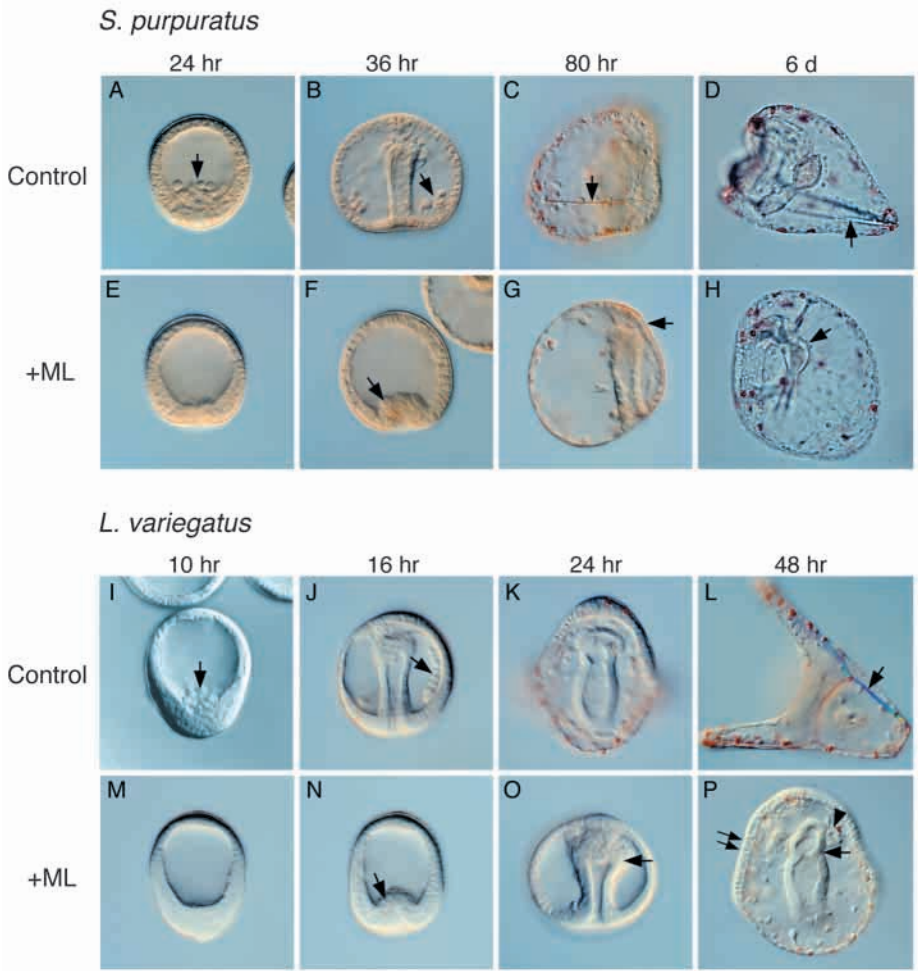

Fig. 4. Effects of Alx1 MOs in *S. purpuratus* (A-H) and *L. variegatus* (I-P). MOs were complementary to non-overlapping regions of the *Spalx1* and *Lvalx1* mRNAs and produced essentially identical phenotypes in the two species. Control embryos show normal PMC ingression (A,I, arrows), PMC migration (B,J, arrows), and skeletogenesis (C,D,K,L, arrows). Alx1 MO-injected embryos lacked PMCs (E,M) and invaginated in a delayed fashion (F,N, arrows). They failed to form skeletal elements even after prolonged culture (H,P). Eventually they developed a tripartite gut (H,P, arrows), pigment cells (see Fig. 5), blastocoelar cells, and coelomic pouches (P, arrowhead). Ectodermal territories appear to differentiate normally (thickened oral ectoderm is indicated by the arrow in G and the double arrow in P). Arrow in O indicates expanded archenteron tip in *L. variegatus* embryos injected with Alx1 MO.

control embryos. Using an anti-myosin heavy chain antibody (Wessel et al., 1990) we found that circumesophageal muscle fibers formed in MO-injected embryos, although in a delayed fashion relative to control sibling embryos (Fig. 5K,L).

Control experiments showed that the MOs were effective in blocking the expression of Alx1 protein and that the observed phenotype resulted specifically from this inhibition. Alx1 MOs blocked nuclear accumulation of Alx1 protein in the large micromere progeny as shown by immunostaining (Fig. 3D). Injection of several other MOs into *S. purpuratus* and *L. variegatus* eggs at the same concentrations did not affect PMC formation or skeletogenesis. As an additional control for specificity, we injected *S. purpuratus* Alx1 MO into *L. variegatus* eggs. The LvAlx1 mRNA and SpAlx1 MO are mismatched at 4/25 nucleotides, a degree of mismatching that has been shown to significantly reduce the effectiveness of a MO directed against globin mRNA (Summerton, 1999). We found that concentrations of SpAlx1 MO that resulted in a robust phenotype in *S. purpuratus* had no effect when injected into *L. variegatus* eggs. Finally, as noted above, SpAlx1 and LvAlx1 MOs produced the same phenotype although they were complementary to non-overlapping regions of the target mRNAs.

Because the phenotype of Alx1 MO-injected embryos resembled in some respects the phenotype of embryos in which early cleavage divisions have been equalized (Langelan and Whiteley, 1985), we performed one experiment to directly test the possibility that the MO might perturb the pattern of early cleavage and micromere formation. We allowed MO-injected *S. purpuratus* embryos to develop to the 16-cell stage, then removed from the dish any that showed signs of abnormal cleavage. The remaining embryos exhibited the same PMC(–) phenotype described above. Although we did not follow the pattern of cell division in the MO-injected embryos after fourth cleavage, these observations suggest that the MO does not affect PMC specification by altering the spatial pattern of early cleavage.

Upstream regulators of Alx1

Beta-catenin function is required for the expression of all mesendoderm-specific mRNAs that have been analyzed to date. This observation, and the fact that the micromeres and their progeny have high levels of nuclear β-catenin (Logan et al., 1999), suggested that activation of Alx1 expression might be dependent on β-catenin. To test this hypothesis, Alx1

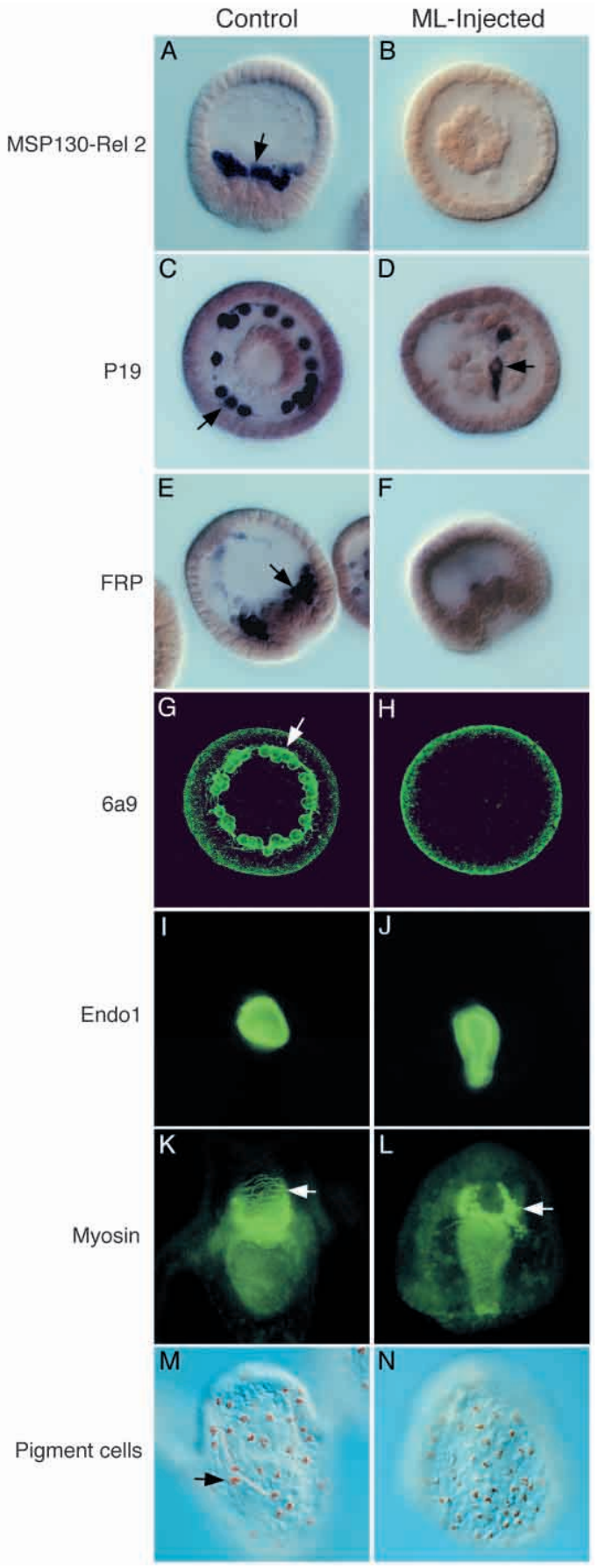

Fig. 5. Effects of Alx1 MOs in *S. purpuratus* (A-H) and *L. variegatus* (I-N). MO-injected embryos were examined 36 hours (B,D,F,H) or 54 hours (J,L,N) postfertilization. (A-F) In situ hybridizations with *SpMSP130-related 2*, *SpP19* and *SpFRP* probes. Control embryos show strong signal in large micromere progeny in the vegetal plate and in PMCs following ingression (A,C,E, arrows) (see also Illies et al., 2002). MO-injected embryos show few or no positive cells. (G,H) Immunostaining with mAb 6a9, showing stained cells (PMCs) in control (G, arrow) but not MO-injected (H) embryos. (I,J) Endo1 expression in the midgut of a control pluteus at 24 hours (note that the hindgut is out of focus) and in the midgut/hindgut of a MO-injected embryo. (K,L) Myosin heavy chain expression in circumesophageal muscle cells (arrows) of a control pluteus (24 hours) and in a MO-injected embryo. (M,N) Pigment cells in the aboral ectoderm of a control (arrow; 48 hours) and a MO-injected embryo.

Table 1. Effect of SpAlx1 MO on levels of various mRNAs as measured by QPCR

Gene	18-20 hour embryos (Alx1 ML, control ML)	23-24 hour embryos (Alx1 ML, control ML)
alx1	2.78, 2.86	3.33, 1.82
tbr	0.65, 0.55	0.55
ets1	0.64, 0.72	0.71, 0.58
dri	0.07, 0.10	0.29
delta	0.85, 0.83	0.90, 0.83
pmar1	1.02, 0.75	ND
msp130	0.22, 0.14	0.31
msp130-rel-2	0.14	ND
sm50	0.38	0.27, 0.11

Numbers shown are fold differences in the expression levels of mRNAs, based on comparisons of embryos injected with Alx1 MO or a control MO. Cycle threshhold (C_T) data obtained by QPCR were first normalized to C_T values for ubiquitin in each sample. Normalized cycle thresholds (ΔC_T) were used to calculate fold differences, with the conservative assumption that the efficiency of amplification was 1.9× per cycle. Fold difference is then $1.9^{\Delta CT}$. For most gene markers, two independent trials were carried out at each of two time points.

Table 2. Effect of overexpression of various proteins on *alx1* mRNA levels as measured by QPCR

Over-expressed proteins	12 hour embryos	24 hour embryos
Pmar1	20.47, 6.61	42.55, 10.21
Cadherin	0.05, 0.01	0.13, 0.07
Cadherin + Pmar1	11.99, 7.04	123.48, 20.06
Cadherin + EnHD	5.04, 1.50	15.77, 4.92
EnHD	4.23, 1.50	6.53, 4.32

Numbers shown are fold differences, calculated as described in the Materials and Methods. Two time points were examined and two independent trials were carried out for each experiment.

expression was assayed in embryos that had been injected with mRNA encoding full-length *Xenopus* C-cadherin (experiments in *L. variegatus*), or the transmembrane/cytoplasmic domain of LvG-cadherin (experiments in *S. purpuratus*). Embryos injected with these cadherin mRNAs lack detectable levels of nuclear β-catenin and exhibit an animalized phenotype (Wikramanayake et al., 1998; Logan et al., 1999). In such embryos, we could detect no nuclear LvAlx1 protein (Fig. 3H) and expression of *Spalx1* was dramatically reduced as assayed by QPCR (Table 2). These experiments demonstrate that zygotic activation of LvAlx1 is dependent on β-catenin.

Pmar1 is a critical early transcriptional regulator in the gene network that controls PMC specification (Oliveri et al., 2002). The first expression of *Spalx1*, detectable by in situ hybridization analysis, followed that of *pmar1* by one cell cycle. These observations raised the possibility that expression of *Spalx1* might be regulated by *pmar1*. Consistent with this hypothesis, we found that overexpression of Pmar1 or an engrailed-pmar1 fusion protein (EnHD) (Oliveri et al., 2002) resulted in a striking increase in levels of *Spalx1* mRNA expression as assayed by QPCR (Table 2). The fact that overexpression of wild-type Pmar1 and EnHD produced similar effects supports the view that Pmar1 normally acts as a repressor (Oliveri et al., 2002). Moreover, we observed that overexpression of Pmar1 (or EnHD) could activate *Spalx1* expression to high levels even in cadherin mRNA-injected embryos (Table 2).

Alx1 and transfating of cells to a skeletogenic fate

In undisturbed embryos, SMCs do not express detectable levels of Alx1 mRNA or protein (Figs 2,3). We tested whether the transfating of SMCs following PMC removal was associated with activation of Alx1 expression. The entire complement of PMCs was removed microsurgically from mesenchyme blastula stage embryos and the resultant PMC(–) embryos were double-immunostained with Alx1 antibody and mAb 6a9 at various times after the operation. Early in the transfating process (i.e., at the late gastrula stage), we observed numerous Alx1-expressing cells at the tip of the archenteron, many of which also stained with mAb 6a9 (Fig. 6). We also observed Alx1-positive cells that were not stained with mAb 6a9. This is consistent with the finding that in normal embryos, expression of Alx1 precedes that of the MSP130 proteins.

As noted above, embryos injected with Alx1 MOs typically failed to form skeletal elements even after prolonged periods in culture. This suggested that Alx1 MOs blocked not only the initial specification of PMCs but the transfating of other cell lineages to a skeletogenic fate. We investigated this further by counting numbers of 6a9(+) cells in *L. variegatus* embryos at different developmental stages after MO injection. In one experiment, separate batches of zygotes from a single fertilization were injected with either 5 or 10 pl of MO injection solution. The relative amounts of injection solution were carefully controlled by delivering either one or two pulses (100 mseconds each) with the picospritzer, using the same microneedle to inject both sets of eggs.

Alx1 MO-injected embryos showed a dose-dependent suppression of the transfating response. In *L. variegatus*, microsurgical removal of micromeres or PMCs leads to the appearance of 60-70 6a9-positive cells 24 hours postfertilization at 23°C (Ettensohn and McClay, 1988; Sweet et al., 1999). Embryos injected with the lower dose of LvAlx1 MO showed greatly reduced numbers of 6a9-positive cells, even after 29 hours of development (mean no. of 6a9-positive cells=26.1, s.d.±9.7, n=20). Embryos injected with the higher dose of MO showed almost complete suppression of transfating at 29 hours (mean no. of 6a9-positive cells=3.3, s.d.±4.1, n=17). The reduced numbers of 6a9-positive cells in

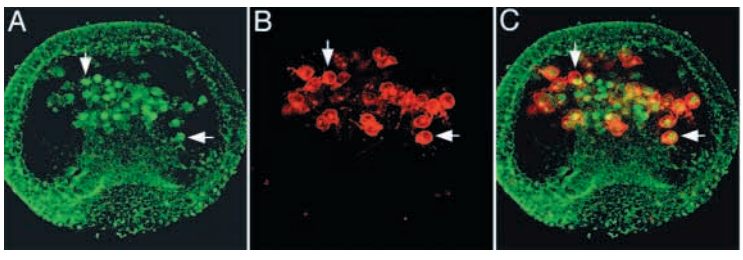

Fig. 6. Activation of Alx1 expression in transfating cells. *L. variegatus* embryos were fixed 10 hours after PMC removal and immunostained with αAlx1 and mAb 6a9. (A) αAlx1 staining. (B) MAb 6a9 staining. (C) Overlay of A and B. 6a9-positive cells also have nuclear Alx1 (arrows). Some Alx1-positive cells are not stained with 6a9, perhaps because they are at an early stage in the transfating process.

MO-injected embryos could not be attributed simply to a delay in transfating. Immunostaining of MO-injected embryos at earlier times showed that transfating began at about 19 hours, as judged by the earliest appearance of faintly stained, 6a9-positive cells in association with the archenteron. This corresponds closely to the time at which transfating is first detectable following microsurgical removal of micromeres [see table 1 in Sweet et al. (Sweet et al., 1999)] or PMCs (Ettensohn and McClay, 1988) when embryos are cultured at 23°C.

DISCUSSION

The developmental function of Alx1

The timing of Alx1 expression and the phenotype of Alx1 MO-injected embryos indicate that this protein functions at an early step in PMC specification. In *S. purpuratus*, *alx1* mRNA expression is detectable specifically in the large micromeres, the founder cells of the PMC lineage, in the first interphase after these cells are born. Inhibition of Alx1 protein expression using MOs blocks the earliest step in PMC morphogenesis (epithelial-mesenchymal transition) as well as the expression of several PMC-specific transcripts normally activated at high levels prior to ingression.

Alx1 MOs produced very limited effects on cell types other than skeletogenic mesoderm. Embryos injected with Alx1 MO gastrulated and subsequently formed a compartmentalized gut and polarized ectoderm. Alx1 MO-injected embryos also formed large numbers of pigment cells. This is in clear contrast to embryos lacking micromeres, which are almost devoid of pigment cells (<5 pigment cells/embryo) (Sweet et al., 1999). Pigment cell specification requires an inductive signal from the large micromeres, a signal recently shown to be the protein Delta (Sweet et al., 2002). The formation of large numbers of pigment cells in Alx1 MO-injected embryos is consistent with QPCR data showing that Alx1 MO has little effect on *Delta* mRNA expression.

Alx1 MO-injected embryos showed a consistent delay in invagination and in the subsequent differentiation of the archenteron. Multiple factors probably contributed to these phenotypic effects. Surgical removal of micromeres at the 16-cell stage delays invagination in both *S. purpuratus* (Ransick and Davidson, 1995) and *L. variegatus* (Sweet et al., 1999). This may reflect an early inductive interaction between micromeres and overlying veg2 cells or a mechanical potentiation of invagination resulting from PMC ingression (see Ransick and Davidson, 1995). It appears that Alx1 protein is expressed too late in cleavage to activate the putative early inducing signal (Ransick and Davidson, 1995). It is more likely, therefore, that the delay in invagination in MO-injected embryos is due to mechanical effects, or possibly to interference with yet another micromere-derived signal, distinct from both Delta and the putative early signal. With respect to the later differentiation of the archenteron, there is evidence that stimulatory signals are produced by PMCs during gastrulation. Removal of PMCs at the mesenchyme blastula stage delays archenteron differentiation without affecting the timing of invagination (Hamada and Kiyomoto, 2000). PMCs normally secrete a variety of proteins into the blastocoel matrix during gastrulation (Zhu et al., 2001) and archenteron differentiation may be regulated by these factors.

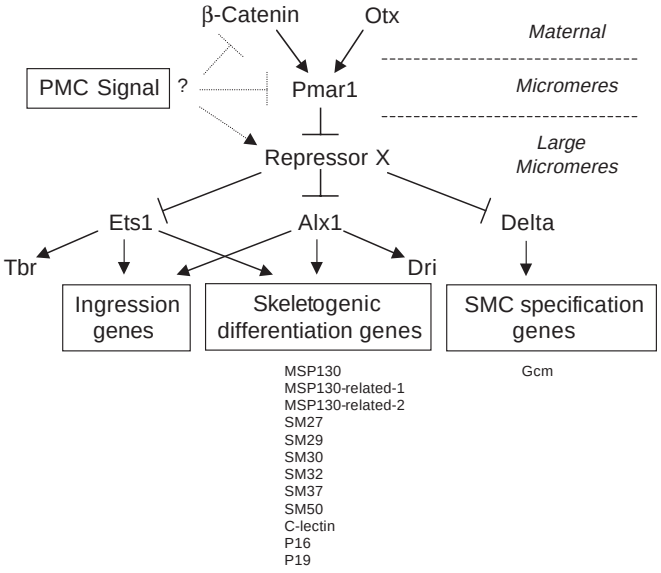

Fig. 7. The micromere-PMC gene regulatory network. The total developmental time represented in the diagram is from fertilization (top) to the blastula stage (bottom). Arrows and bars indicate positive and negative interactions, respectively. All genes shown encode transcription factors with the exception of *Delta*, which encodes a transmembrane protein. There is evidence for a direct interaction between Ets1 and *sm50* (Kurokawa et al., 1999) but all other interactions may be indirect. β-catenin and Otx are maternal proteins that become differentially enriched in micromere nuclei at the 16-cell stage (Chuang et al., 1996; Logan et al., 1999). These two proteins are required for the activation of *pmar1*, which is expressed only by the micromeres and their progeny (Oliveri et al., 2002). Pmar1 may block the expression of a putative repressor (Repressor X) specifically in the micromeres. This repressor (which may be several proteins) blocks PMC fate specification in all non-micromere lineages (Oliveri et al., 2002). *Ets1*, *alx1* and *delta* are all regulated independently by pmar1 and the repressor. Ets1 regulates the *tbr* gene (Fuchikami et al., 2002) and Alx1 regulates *dri* (this study). Alx1, Ets1 and Tbr are all expressed only by the large micromeres and their progeny. Alx1 and Ets1 both regulate genes involved in ingression and skeletogenesis (Kurokawa et al., 1999; this paper). Delta signaling activates genes involved in SMC specification, including *gcm* (Ransick et al., 2002; Sweet et al., 2002). PMC signals feed into the network upstream of *alx1* (this study); dashed bars and dashed arrow show possible inputs.

The PMC gene network

Based on the present study and other recent work (Kurokawa et al., 1999; Zhu et al., 2001; Davidson et al., 2002; Fuchikami et al., 2002; Illies et al., 2002; Oliveri et al., 2002), a framework of the gene network that controls PMC specification can now be constructed (Fig. 7). Maternal inputs into this network lead ultimately to the activation or repression of genes that control the complex morphogenetic behaviors of PMCs (ingression, migration and cell fusion) and their terminal differentiation into biomineral-forming cells.

Our results show that Pmar1 and its upstream regulator, β-catenin, are positive regulators of Alx1 expression. In *S. purpuratus*, *alx1* transcript begins to accumulate in the first interphase after the large micromeres are born. This is just one cell cycle after β-catenin begins to accumulate in the nuclei of micromeres (Logan et al., 1999) and activates the expression

of *pmar1* (Oliveri et al., 2002). We found that overexpression of Pmar1 dramatically elevated *alx1* mRNA levels even in cadherin mRNA-injected embryos. This suggests that the regulation of *alx1* expression by β-catenin may be mediated solely through *pmar1* (Fig. 7). If there are other inputs from β-catenin to *alx1*, they are dispensable in the presence of high levels of Pmar1. Pmar1 is a transcriptional repressor and probably acts indirectly on *alx1* by blocking the expression of an unidentified repressor (Oliveri et al., 2002) (this work). It is noteworthy that although *pmar1* mRNA is expressed in both daughter cells of the micromeres, an unknown mechanism restricts *alx1* expression to the large micromeres. Pmar1 may not block the expression of the putative repressor in small micromeres or there may be other mechanisms that prevent Alx1 expression in these cells.

Injection of *pmar1* mRNA causes mesomeres to adopt a PMC-like fate (P. Oliveri and D. McClay, personal communcation). In contrast, overexpression of *alx1* mRNA is insufficient to convert other cell lineages to a skeletogenic fate (data not shown). *Pmar1* is therefore likely to control key regulators of PMC fate specification other than *alx1*, probably including other transcription factors expressed selectively or exclusively by the large micromere lineage. Zygotic expression of *ets1* is restricted to the large micromere lineage in *Hemicentrotus pulcherrimus* (Kurokawa et al., 1999), although in *L. variegatus* this gene is expressed by both PMCs and SMCs (X. Zhu and C.A.E., unpublished observations). Zygotic expression of *tbr* is restricted to the large micromere lineage (Croce et al., 2001; Fuchikami et al., 2002). *Alx1* is expressed earlier than either *ets1* or *tbr* but our QPCR studies suggest it is not required for the expression of either gene (Table 1 and Fig. 7). *Dri*, another transcriptional regulator expressed by PMCs (G. Amore and E. Davidson, personal communication) is regulated positively by *alx1* (Fig. 7).

Alx1 is required for at least two distinct morphogenetic processes in the large micromere lineage: (1) ingression (epithelial-mesenchymal transition) and (2) skeletogenesis. The molecular changes required for ingression have not yet been identified, although this process is associated with changes in cell shape, protrusive activity, adhesive properties and cell surface architecture (Fink and McClay, 1985; Miller and McClay, 1997). In contrast, a large number of terminal differentiation gene products have been identified that function in the formation of the biomineralized skeleton (see Illies et al., 2002; Wilt, 2002) (Fig. 7). These gene products are expressed specifically in the large micromere lineage beginning at the mid-late blastula stage, prior to PMC ingression. We examined the expression of four such markers in this study, SpMSP130, SpMSP130-related 2, SpP19 and SpSM50, and found that all four are regulated positively by Alx1. This suggests that Alx1 is a key regulator of the molecular subprogram that controls skeletogenesis.

Activation of the PMC gene network through a regulative pathway: different upstream inputs lead to the same output

Our MO studies show that Alx1 is essential not only for normal PMC specification but also for the transfating of non-micromere lineages to a skeletogenic fate. The most likely explanation is that Alx1 is required in the transfating cells. In support of this view, we have shown that *Alx1* (Results) and several of its downstream targets (Guss, 1997) are selectively activated in the transfating cells. There are other possible interpretations of our transfating experiments that would involve a role for Alx1 in the micromeres, but these can be excluded based on other experimental data. For example, an early, Alx1-dependent signal from large micromeres might be required for veg2-derived cells to become competent to transfate. This is clearly not the case, however, as a robust transfating response is observed when micromeres are removed from 16-cell stage embryos, prior to the onset of Alx1 expression (Sweet et al., 1999). Another possibility is that in MO-injected embryos, the large micromere progeny continue to provide the signal that suppresses transfating, either because the signal is independent of Alx1 or because levels of the MO are too low to effectively block the signal. Neither scenario is consistent with the dose-dependent effect of the MOs, however. For example, if MOs were only partially blocking the PMC-derived signal then higher concentrations would be more effective and lead to greater numbers of transfating cells. In fact, the opposite was observed. We conclude that Alx1 is required in the transfating cells where it functions to regulate key subprograms within the PMC gene network.

The PMC gene network is activated in different ways in transfating cells and large micromeres. Transfating cells activate the network by a mechanism responsive to cell signaling, whereas in large micromeres the pathway is activated via a signal-independent, maternal mechanism that concentrates β-catenin in micromere nuclei (Ettensohn and Sweet, 2000; Brandhorst and Klein, 2002; Angerer and Angerer, 2003). Our findings show that the divergence in the normal and regulative pathways lies upstream of *alx1* (Fig. 7). Despite different upstream inputs, the gene regulatory network downstream of Alx1 in transfating cells and large micromeres appears to be identical.

The Cart1/Alx3/Alx4 subfamily and the evolution of biomineralization

The primary sequence of the Sp/LvAlx1 homeodomain indicates that this protein is the first invertebrate member of the Cart1/Alx3/Alx4 family of Paired-class homeodomain proteins. In our molecular phylogenetic analysis, the Sp/LvAlx1 homeodomain clustered with this gene family even when only the most closely related Paired-class homeodomain subfamilies were included (Fig. 1B) (Galliot et al., 1999). There are also similarities between Sp/LvAlx1 and members of the Cart1/Alx3/Alx4 family outside the homeodomain; viz., the presence of a charged domain upstream of the homeodomain, a C-terminal OAR domain, and an overall abundance of proline residues.

In vertebrates, the Cart1/Alx3/Alx4 proteins have been implicated in the formation of the limb skeleton and the neural crest-derived skeleton of the face and neck. These three genes are expressed in similar patterns by neural crest-derived mesenchyme of developing craniofacial regions and by the mesenchyme of developing limbs (Zhao et al., 1994; Qu et al., 1997; ten Berge et al., 1998; Beverdam and Meijlink, 2001). Mice with compound mutations in Alx3 and Alx4 have severe defects in neural crest-derived skeletal elements (Beverdam et al., 2001). Alx4/Cart1 double mutants have a similar phenotype (Qu et al., 1999) (see Beverdam et al., 2001). In humans, mutations in ALX4 have been shown to cause defects in skull

ossification (Wu et al., 2000; Mavrogiannis et al., 2001). Alx4 and Cart1 appear to recognize identical palindromic sites on DNA and bind to these sites as homo- or heterodimers (Qu et al., 1999). In vertebrates, it is not yet clear whether these proteins function primarily in fate specification, cell death, division, or other developmental processes.

The fact that similar proteins are involved in skeletogenesis in sea urchins and vertebrates raises the possibility there might be an evolutionary link between certain features of skeleton formation in these two groups of deuterostomes. It has been proposed that the ancestral deuterostome (the most recent common ancestor of echinoderms, hemichordates and chordates) may have had an extensive calcitic skeleton much like that of modern sea urchins (Jefferies et al., 1996; Dominguez et al., 2002). This controversial hypothesis is based partly on the interpretation of paleozoic fossils known as mitrates – bilaterally symmetrical organisms that possessed gill-slits and large, calcitic tests. Similarities among proteins associated with the biominerals of echinoderms and other animals suggest that certain features of biomineralization may have even more ancient origins, i.e., predating the deuterostome-protostome split. For example, C-lectin domain-containing proteins have recently been shown to be associated with biominerals of echinoderms, molluscs and vertebrates (Mann and Siedler, 1999; Mann et al., 2000; Illies et al., 2002). One hypothesis is that biological calcifying systems in various metazoans (e.g., corals, crustaceans, molluscs, echinoderms and vertebrates) all originated from a common, pre-existing system that initially functioned to suppress mineral deposition in the Neoproterozoic marine environment, which was probably saturated with $CaCO_3$ (Marin et al., 1996; Westbroek and Marin, 1998). Our findings support the view that the ancestral deuterostome possessed a mesenchymal cell lineage that engaged in biomineralization, and that an Alx1-like protein was involved in the specification these cells. Such a primordial cell lineage may have been utilized in a variety of ways during deuterostome evolution to contribute to biomineralized structures in different animals.

We thank M. Peeler for performing Alx1 northern blots, G. Wessel and D. McClay for antibodies, and the anonymous reviewers for their comments. This research was supported by NSF Grant IBN-0128140 to C.A.E. D. DeJong received support from a Carnegie Mellon SURG grant.

REFERENCES

Amendt, B. A., Sutherland, L. B. and Russo, A. F. (1999). Multifunctional role of the Pitx2 homeodomain protein C-terminal tail. *Mol. Cell. Biol.* **19**, 7001-7010.

Angerer, L. M. and Angerer, R. C. (2003). Patterning the sea urchin embryo: gene regulatory networks, signaling pathways, and cellular interactions. *Curr. Top. Dev. Biol*. **53**, 159-198.

Banerjee-Basu, S. and Baxevanis, A. D. (2001). Molecular evolution of the homeodomain family of transcription factors. *Nucl. Acid. Res.* **29**, 3258-3269.

Beverdam, A., Brouwer, A., Reijnen, M., Korving, J. and Meijlink, F. (2001). Severe nasal clefting and abnormal embryonic apoptosis in Alx3/Alx4 double mutant mice. *Development* **128**, 3975-3986.

Beverdam, A. and Meijlink, F. (2001). Expression patterns of group-I aristaless-related genes during craniofacial and limb development. *Mech. Dev.* **107**, 163-167.

Brandhorst, B. P. and Klein, W. H. (2002). Molecular patterning along the sea urchin animal-vegetal axis. *Int. Rev. Cytol*. **213**, 183-232.

Brouwer, A., ten Berge, D., Wiegerinck, R. and Meijlink, F. (2003). The OAR/aristaless domain of the homeodomain protein Cart1 has an attenuating role in vivo. *Mech. Dev.* **120**, 241-252.

Chuang, C. K., Wikramanayake, A. H., Mao, C. A., Li, X. and Klein, W. H. (1996). Transient appearance of Strongylocentrotus purpuratus Otx in micromere nuclei: cytoplasmic retention of SpOtx possibly mediated through an alpha-actinin interaction. *Dev. Genet.* **19**, 231-237.

Croce, J., Lhomond, G., Lozano, J. C. and Gache, C. (2001). ske-T, a T-box gene expressed in the skeletogenic mesenchyme lineage of the sea urchin embryo. *Mech. Dev.* **107**, 159-162.

Davidson, E. H., Rast, J. P., Oliveri, P., Ransick, A., Calestani, C., Yuh, C. H., Minokawa, T., Amore, G., Hinman, V., Arenas-Mena, C., Otim, O., Brown, C. T., Livi, C. B., Lee, P. Y., Revilla, R., Schilstra, M. J., Clarke, P. J., Rust, A. G., Pan, Z., Arnone, M. I., Rowen, L., Cameron, R. A., McClay, D. R., Hood, L. and Bolouri, H. (2002). A provisional regulatory gene network for specification of endomesoderm in the sea urchin embryo. *Dev. Biol.* **246**, 162-190.

Dominguez, P., Jacobson, A. G. and Jefferies, R. P. (2002). Paired gill slits in a fossil with a calcite skeleton. *Nature* **417**, 841-844.

Emily-Fenouil, F., Ghiglione, C., Lhomond, G., Lepage, T. and Gache, C. (1998). GSK3beta/shaggy mediates patterning along the animal-vegetal axis of the sea urchin embryo. *Development* **125**, 2489-2498.

Ettensohn, C. A. (1992). Cell interactions and mesodermal cell fates in the sea urchin embryo. *Development* **Suppl.** 43-51.

Ettensohn, C. A. and McClay, D. R. (1988). Cell lineage conversion in the sea urchin embryo. *Dev. Biol*. **125**, 396-409.

Ettensohn, C. A. and Ruffins, S. W. (1993). Mesodermal cell interactions in the sea urchin embryo: properties of skeletogenic secondary mesenchyme cells. *Development* **117**, 1275-1285.

Ettensohn, C. A. and Sweet, H. C. (2000). Patterning the early sea urchin embryo. *Curr. Top. Dev. Biol*. **50**, 1-44.

Fink, R. D. and McClay, D. R. (1985). Three cell recognition changes accompany the ingression of sea urchin primary mesenchyme cells. *Dev. Biol*. **107**, 66-74.

Fuchikami, T., Mitsunaga-Nakatsubo, K., Amemiya, S., Hosomi, T., Watanabe, T., Kurokawa, D., Kataoka, M., Harada, Y., Satoh, N., Kusunoki, S., Takata, K., Shimotori, T., Yamamoto, T., Sakamoto, N., Shimada, H. and Akasaka, K. (2002). T-brain homologue (HpTb) is involved in the archenteron induction signals of micromere descendant cells in the sea urchin embryo. *Development* **129**, 5205-5216.

Galliot, B., de Vargas, C. and Miller, D. (1999). Evolution of homeobox genes: Q50 Paired-like genes founded the Paired class. *Dev. Genes Evol.* **209**, 186-197.

Gibson, A. W. and Burke, R. D. (1985). The origin of pigment cells in embryos of the sea urchin Strongylocentrotus purpuratus. *Dev. Biol.* **107**, 414-419.

Guss, K. A. (1997). *An Analysis of Gene Expression During Skeletal Morphogenesis in the Sea Urchin Embryo*. PhD thesis, Carnegie Mellon University.

Hamada. M. and Kiyomoto, M. (2000). Primary mesenchyme cells play an important role in determining the timing of endoderm-specific alkaline phosphatase expression. *Zool. Sci*. **17 Supplement**, 67.

Hodor, P. G., Illies, M. R., Broadley, S. and Ettensohn, C. A. (2000). Cell-substrate interactions during sea urchin gastrulation: migrating primary mesenchyme cells interact with and align extracellular matrix fibers that contain ECM3, a molecule with NG2-like and multiple calcium-binding domains. *Dev. Biol*. **222**, 181-194.

Huang, L., Li, X., El-Hodiri, H. M., Dayal, S., Wikramanayake, A. H. and Klein, W. H. (2000). Involvement of Tcf/Lef in establishing cell types along the animal-vegetal axis of sea urchins. *Dev. Genes Evol*. **210**, 73-81.

Illies, M. R., Peeler, M. T., Dechtiaruk, A. M. and Ettensohn, C. A. (2002). Identification and developmental expression of new biomineralization proteins in the sea urchin, *Strongylocentrotus purpuratus*. *Dev. Genes Evol.* **212**, 419-431.

Jefferies, R. P. S., Brown, N. A. and Daley, P. E. J. (1996). The early phylogeny of chordates and echinoderms and the origin of chordate left-right asymmetry and bilateral symmetry. *Acta Zool.* (Stockholm) **77**, 101-122.

Katoh-Fukui, Y., Noce, T., Ueda, T., Fujiwara, Y., Hashimoto, N., Higashinakagawa, T., Killian, C. E., Livingston, B. T., Wilt, F. H., Benson, S. C., Sucov, H. M. and Davidson, E. H. (1991). The corrected structure of the SM50 spicule matrix protein of Strongylocentrotus purpuratus. *Dev. Biol*. **145**, 201-202.

Kurokawa, D., Kitajima, T., Mitsunaga-Nakatsubo, K., Amemiya, S.,

Shimada, H. and Akasaka, K. (1999). HpEts, an ets-related transcription factor implicated in primary mesenchyme cell differentiation in the sea urchin embryo. *Mech. Dev.* **80**, 41-52.

Langelan, R. E. and Whiteley, A. H. (1985). Unequal cleavage and the differentiation of echinoid primary mesenchyme. *Dev. Biol.* **109**, 464-475.

Logan, C. Y., Miller, J. R., Ferkowicz, M. J. and McClay, D. R. (1999). Nuclear beta-catenin is required to specify vegetal cell fates in the sea urchin embryo. *Development* **126**, 345-357.

Mann, K. and Siedler, F. (1999). The amino acid sequence of ovocleidin 17, a major protein of the avian eggshell calcified layer. *Biochem. Mol. Biol. Int.* **47**, 997-1007.

Mann, K., Weiss, I. M., Andre, S., Gabius, H. J. and Fritz, M. (2000). The amino-acid sequence of the abalone (Haliotis laevigata) nacre protein perlucin. Detection of a functional C-type lectin domain with galactose/mannose specificity. *Eur. J. Biochem.* **267**, 5257-5264.

Marin, F., Smith, M., Isa, Y., Muyzer, G. and Westbroek, P. (1996). Skeletal matrices, muci, and the origin of invertebrate calcification. *Proc. Natl. Acad. Sci. USA* **93**, 1554-1559.

Mavrogiannis, L. A., Antonopoulou, I., Baxova, A., Kutilek, S., Kim, C. A., Sugayama, S. M., Salamanca, A., Wall, S. A., Morriss-Kay, G. M., Wilkie, A. O. (2001). Haploinsufficiency of the human homeobox gene ALX4 causes skull ossification defects. *Nat. Genet.* **27**, 17-18.

Miller, J. R. and McClay, D. R. (1997). Characterization of the role of cadherin in regulating cell adhesion during sea urchin development. *Dev. Biol.* **192**, 323-339.

Norris, R. A. and Kern, M. J. (2001). The identification of Prx1 transcription regulatory domains provides a mechanism for unequal compensation by the Prx1 and Prx2 loci. *J. Biol. Chem.* **276**, 26829-26837.

Oliveri, P., Carrick, D. M. and Davidson, E. H. (2002). A regulatory gene network that directs micromere specification in the sea urchin embryo. *Dev. Biol.* **246**, 209-228.

Parr, B. A., Parks, A. L. and Raff, R. A. (1990). Promoter structure and protein sequence of msp130, a lipid-anchored sea urchin glycoprotein. *J. Biol. Chem.* **265**, 1408-1413.

Qu, S., Li, L. and Wisdom, R. (1997). Alx-4: cDNA cloning and characterization of a novel paired-type homeodomain protein. *Gene* **203**, 217-223.

Qu, S., Tucker, S. C., Zhao, Q., deCrombrugghe, B. and Wisdom, R. (1999). Physical and genetic interactions between Alx4 and Cart1. *Development* **126**, 359-369.

Ransick, A. and Davidson, E. H. (1995). Micromeres are required for normal vegetal plate specification in sea urchin embryos. *Development* **121**, 3215-3222.

Ransick, A., Rast, J. P., Minokawa, T., Calestani, C. and Davidson, E. H. (2002). New early zygotic regulators expressed in endomesoderm of sea urchin embryos discovered by differential array hybridization. *Dev. Biol.* **246**, 132-147.

Rast, J. P., Amore, G., Calestani, C., Livi, C. B., Ransick, A. and Davidson, E. H. (2000). Recovery of developmentally defined gene sets from high-density cDNA macroarrays. *Dev. Biol.* **228**, 270-286.

Rozen, S. and Skaletsky, H. J. (2000). Primer3 on the WWW for general users and for biologist programmers. In *Bioinformatics. Methods and Protocols* (ed. S. Krawtz and S. Misener) Methods in Molecular Biology. pp. 365-386. Totowa NJ: Humana Press.

Smith, A. B. (1988). Phylogenetic relationships, divergence times, and rates of molecular evolution for camarodont sea urchins. *Mol. Biol. Evol.* **5**, 345-365.

Summers, R. G., Morrill, J. B., Leith, A., Marko, M., Piston, D. W. and Stonebraker, A. T. (1993). A stereometric analysis of karyokinesis, cytokinesis, and cell arrangements during and following fourth cleavage period in the sea urchin, *Lytechinus variegatus*. *Dev. Growth Differ.* **35**, 41-57.

Summerton, J. (1999). Morpholino antisense oligomers: the case for an RNase H-independent structural type. *Biochim. Biophys. Acta* **1489**, 141-158.

Sweet, H. C., Hodor, P. G. and Ettensohn, C. A. (1999). The role of micromere signaling in Notch activation and mesoderm specification during sea urchin embryogenesis. *Development* **126**, 5255-5265.

Sweet, H. C., Gehring, M. and Ettensohn, C. A. (2002). LvDelta is a mesoderm-inducing signal in the sea urchin embryo and can endow blastomeres with organizer-like properties. *Development* **129**, 1945-1955.

ten Berge, D., Brouwer, A., el Bahi, S., Guenet, J. L., Robert, B. and Meijlink, F. (1998). Mouse Alx3: an aristaless-like homeobox gene expressed during embryogenesis in ectomesenchyme and lateral plate mesoderm. *Dev. Biol.* **199**, 11-25.

Vonica, A., Weng, W., Gumbiner, B. M. and Venuti, J. M. (2000). TCF is the nuclear effector of the beta-catenin signal that patterns the sea urchin animal-vegetal axis. *Dev. Biol.* **217**, 230-243.

Wessel, G. M. and McClay, D. R. (1985). Sequential expression of germ-layer specific molecules in the sea urchin embryo. *Dev. Biol.* **111**, 451-463.

Wessel, G. M., Zhang, W. and Klein, W. H. (1990). Myosin heavy chain accumulates in dissimilar cell types of the macromere lineage in the sea urchin embryo. *Dev. Biol.* **140**, 447-454.

Westbroek, P. and Marin, F. (1998). A marriage of bone and nacre. *Nature* **392**, 861-862.

Wikramanayake, A. H., Huang, L. and Klein, W. H. (1998). Beta-catenin is essential for patterning the maternally specified animal-vegetal axis in the sea urchin embryo. *Proc. Natl. Acad. Sci. USA* **95**, 9343-9348.

Wilt, F. H. (2002). Biomineralization of the spicules of sea urchin embryos. *Zool. Sci.* **19**, 253-261.

Wu, Y. Q., Badano, J. L., McCaskill, C., Vogel, H., Potocki, L., Shaffer, L. G. (2000). Haploinsufficiency of ALX4 as a potential cause of parietal foramina in the 11p11.2 contiguous gene-deletion syndrome. *Am. J. Hum. Genet.* **67**, 1327-1332.

Zhao, G. Q., Eberspaecher, H., Seldin, M. F. and de Crombrugghe, B. (1994). The gene for the homeodomain-containing protein Cart-1 is expressed in cells that have a chondrogenic potential during embryonic development. *Mech. Dev.* **48**, 245-254.

Zhu, X., Mahairas, G., Illies, M., Cameron, R. A., Davidson, E. H. and Ettensohn, C. A. (2001). A large-scale analysis of mRNAs expressed by primary mesenchyme cells of the sea urchin embryo. *Development* **128**, 2615-2627.